Breast ultrasound tomography with two parallel transducer arrays

Lianjie Huang, Junseob Shin, Ting Chen, Youzuo Lin, Kai Gao, Miranda Intrator, Kenneth Hanson

Los Alamos National Laboratory, MS D452, Los Alamos, NM 87545, USA

ABSTRACT

Breast ultrasound tomography is an emerging imaging modality to reconstruct the sound speed, density, and ultrasound attenuation of the breast in addition to ultrasound reflection/beamforming images for breast cancer detection and characterization. We recently designed and manufactured a new synthetic-aperture breast ultrasound tomography prototype with two parallel transducer arrays consisting of a total of 768 transducer elements. The transducer arrays are translated vertically to scan the breast in a warm water tank from the chest wall/axillary region to the nipple region to acquire ultrasound transmission and reflection data for whole-breast ultrasound tomography imaging. The distance of these two ultrasound transducer arrays is adjustable for scanning breasts with different sizes. We use our breast ultrasound tomography prototype to acquire phantom and *in vivo* patient ultrasound data to study its feasibility for breast imaging. We apply our recently developed ultrasound imaging and tomography algorithms to ultrasound data acquired using our breast ultrasound tomography system. Our *in vivo* patient imaging results demonstrate that our breast ultrasound tomography can detect breast lesions shown on clinical ultrasound and mammographic images.

Keywords: Breast cancer, reflection, sound speed, synthetic-aperture ultrasound, transmission, ultrasound attenuation, ultrasound imaging, ultrasound tomography.

1. INTRODUCTION

Breast cancer is the second-leading cause of cancer death among American women. The breast cancer mortality rate in the U.S. changed little from 1930s-1990s, and has decreased only approximately 20% since the 1990s. The mortality rates for many other cancers have been greatly reduced since 1930s. There is an urgent need to improve the sensitivity and specificity of breast cancer imaging to reduce the breast cancer mortality rate.

Estimates of the sensitivity of mammography range from 68% to 88% with specificity from 82% to 98%.[1] However, in radiographically dense breasts, sensitivity can be as low as 30 to 48% because the normal breast parenchyma and stroma mask the presence of masses. Dense breast tissue is common: approximately 50% of women younger than 50 years and a third of older women have dense parenchyma and stroma;[2] these are the very women for whom the risk of developing breast cancer is the highest. As a result, the positive predictive value or PPV (the probability of having cancer for a woman with a positive test) of a biopsy recommendation ranges from 20% in women under age 50 to 60% to 80% in women aged 50-69. PPV of 20% means that 80% of the abnormal findings with mammography turn out to be benign. False positive findings in current breast cancer screenings result in a cost of $2 billion each year for unnecessary biopsies. Moreover, the compression of the breast required during mammography may cause extreme discomfort and apprehension in patients,[3] but is necessary to prevent overlapping of the breast tissue that could mask the presence of a mass on the mammogram. In addition, the use of ionizing radiation limits the frequency of examinations, and the exposure to X-ray mammography for younger women is currently not justified.

Because none of existing clinical imaging modalities can approach the ideal 100% sensitivity and specificity, a vast number of alternative approaches to breast cancer imaging are being investigated. Ultrasound tomography (UST) was developed as a potential quantitative imaging tool in 1970s with the pioneering work of Greenleaf et al.[4,5] and Carson et al.[6] A number of UST prototype systems were developed to study the imaging capability of UST for breast cancer detection and characterization.[7–14] In contrast to mammography, ultrasound can be used in dense breasts, and ultrasound tomography is a safe (non-ionizing radiation) and comfortable (no compression) imaging modality. Synthetic-aperture ultrasound acquires ultrasound reflection/transmission data of ultrasound waves propagating along various directions.[15–22] Using synthetic-aperture ultrasound can improve medical ultrasound imaging and tomography.[12,14,19–46]

Send correspondence to Lianjie Huang: ljh@lanl.gov

Medical Imaging 2016: Physics of Medical Imaging, edited by Despina Kontos, Thomas G. Flohr, Joseph Y. Luo,
Proc. of SPIE Vol. 9783, 97830C · © 2016 SPIE · CCC code: 1605-7422/16/$18 · doi: 10.1117/12.2216531

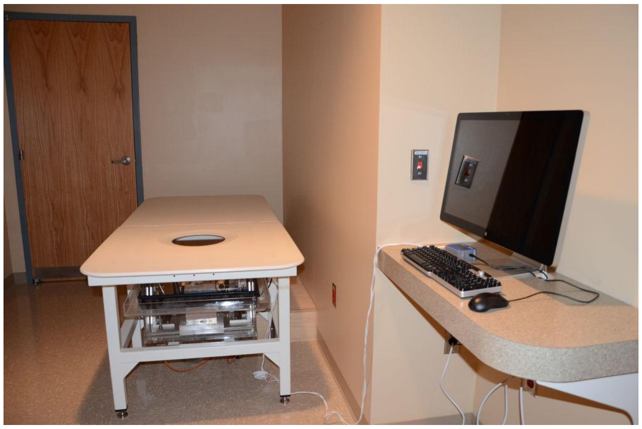

(a) UST scan bed for patient to lie on the bed in the prone position

(b) Data acquisition system

Figure 1: LANL's custom-built breast ultrasound tomography prototype installed in a clinical exam room in the building of the University of New Mexico Outpatient Surgery-Imaging Services in Albuquerque, NM. The prototype consists of 768 ultrasound transducer elements and 384 parallel receive channels for acquiring synthetic-aperture ultrasound transmission and reflection data. (LANL: Los Alamos National Laboratory)

Ultrasound tomography algorithms can be developed using either ray theory or wave theory. The ray-based ultrasound tomography is high-frequency asymptotic approximation of wave-based methods. Ultrasound bent-ray tomography reconstructs the sound-speed and ultrasound attenuation distributions within the breast.[11,43,44,47–57] One of the primary advantages of ultrasound bent-ray tomography is its computational efficiency that could lead to almost real-time imaging using GPU computers.[44]

Ultrasound waveform tomography can properly handle complex wave phenomena in heterogeneous, dense breasts. With the increasing computing power, ultrasound waveform tomography is becoming feasible. We recently developed a suite of novel ultrasound waveform tomography algorithms for improving the robustness and computational efficiency of high-resolution and high-fidelity tomographic reconstructions.[42,46,58–62]

We recently designed and manufactured a synthetic-aperture ultrasound tomography prototype with two parallel ultrasound transducer arrays for studying the clinical feasibility of breast ultrasound tomography.[14] The distance between the two transducer arrays is adjustable for scanning different sizes of breasts. We used our breast ultrasound tomography prototype to scan patients at the University of New Mexico Outpatient Surgery-Imaging Services in Albuquerque, NM, and acquire synthetic-aperture ultrasound transmission and reflection data for ultrasound imaging and tomography.

We briefly describe our custom-built breast ultrasound tomography prototype, give a concise overview on how ultrasound reflection data can improve ultrasound waveform tomography and on our recent work on ultrasound attenuation tomography, and present present some *in vivo* patient imaging examples to demonstrate that our breast ultrasound tomography prototype with two parallel transducer arrays can detect breast lesions shown on clinical ultrasound and mammographic images.

2. BREAST ULTRASOUND TOMOGRAPHY PROTOTYPE

The advanced technologies in manufacture of large ultrasound transducer arrays, real-time data acquisition for synthetic-aperture ultrasound, computer memory for real-time data storage, solid state drives for quickly storage of a large amount of synthetic-aperture ultrasound data, and parallel computing for high-resolution image reconstruction, enable us to build a synthetic-aperture breast ultrasound tomography system for clinical studies. We recently designed and manufactured a synthetic-aperture breast ultrasound tomography prototype for the *in vivo* patient study using parts from various companies.[14] Fig. 1 shows the breast ultrasound tomography prototype that was installed in a clinical exam room in the building of the University of New Mexico (UNM) Outpatient Surgery-Imaging Services in Albuquerque, NM, for acquiring patient ultrasound tomography data. The prototype consists of two parallel transducer arrays (Fig. 2a), a motion control system with two linear motion stages, a warm water imaging tank, a storage water tank with warm water, a water filtering system,

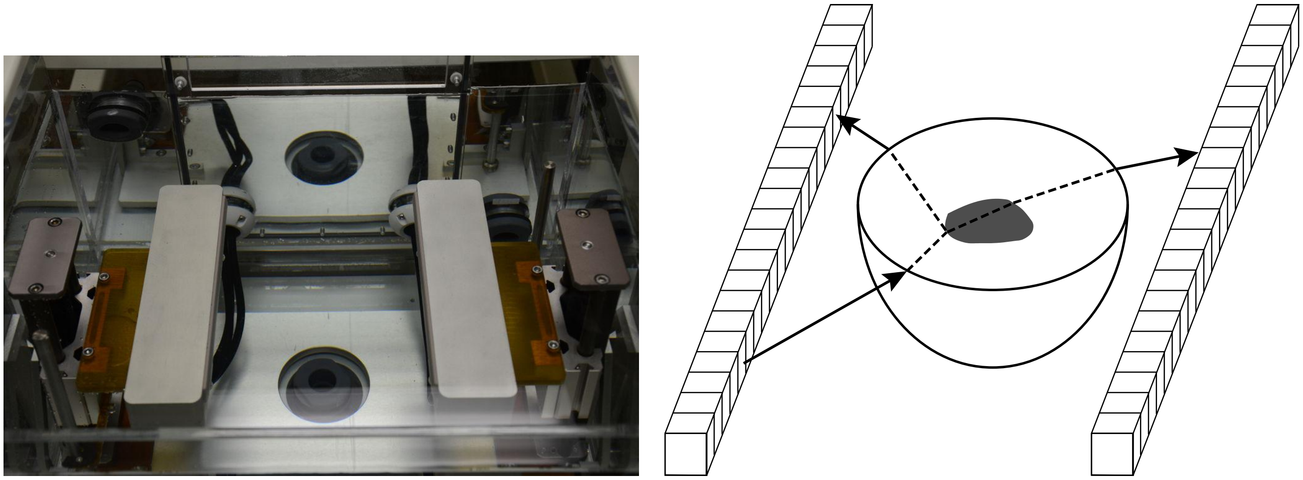

(a) (b)

Figure 2: Two parallel ultrasound transducer arrays (a) used in LANL's custom-built breast ultrasound tomography prototype and (b) schematic illustration of ultrasound reflection and transmission.

a water degassing system, a data acquisition system, a master PC computer to control the operation of the entire system, and an exam table for patients to lie down in the prone position for ultrasound tomography scanning.

The two parallel transducer arrays (Fig. 2a) consists of a total of 768 transducer elements firing ultrasound at the center frequency of 1.875 MHz. The distance between the two parallel transducer arrays is adjustable to optimally scan breasts with different sizes. The ultrasound transducer arrays are translated vertically to scan the whole breast from the chest wall/axillary region to the nipple region. The system acquires ultrasound reflection and transmission data simultaneously (Fig. 2b). The 768-channel Verasonics data acquisition system uses 384 parallel receive channels to record synthetic-aperture ultrasound data: Each transducer element is fired sequentially, and all transducer elements receive ultrasound transmission/reflection/scattering signals. It takes approximately 2.5 seconds to scan one slice, including times to move and align the two ultrasound transducer arrays, scan the breast, and store synthetic-aperture ultrasound data to solid state hard drives for ultrasound imaging and tomography.

3. ULTRASOUND TOMOGRAPHY WITH BOTH TRANSMISSION AND REFLECTION DATA

Tomography often uses only transmission data. Ultrasound reflection data carry high-frequency spatial information of the breast, and ultrasound reflection imaging often generates high-resolution images. In recent years, we developed a suite of novel ultrasound ray and waveform tomography algorithms,[42–44,46,56–62] and demonstrated that ultrasound reflection data can improve ultrasound waveform tomography (USWT), as shown in Fig. 3.[45] The numerical phantom in Fig. 3(a) contains two small tumors with diameters of 2 mm and 8 mm, respectively. Numerical synthetic-aperture ultrasound data are generated for two parallel ultrasound transducer arrays on the top and bottom sides of the numerical phantom. The USWT reconstruction with ultrasound transmission data alone cannot separate the two small tumors, as shown in Fig. 3(b), while the USWT reconstruction using ultrasound reflection alone as displayed in Fig. 3(c) can clearly separate the two small tumors but cannot fully reconstruct the larger tumor. In contrast, USWT with both ultrasound transmission and reflection data can well reconstruct the two small tumors, as depicted in Fig. 3(d).

Figure 4 demonstrates using a chicken phantom dataset acquired with our synthetic-aperture ultrasound tomography prototype that ultrasound waveform tomography with both ultrasound transmission and reflection data can reconstruct the inhomogeneous sound-speed distribution within the two pieces of chicken breast.[62] The tomographic image in Figure 4(b) is obtained using the ultrasound waveform tomography method with the second-order total-generalized-variation regularization developed by Lin and Huang (2016).[62]

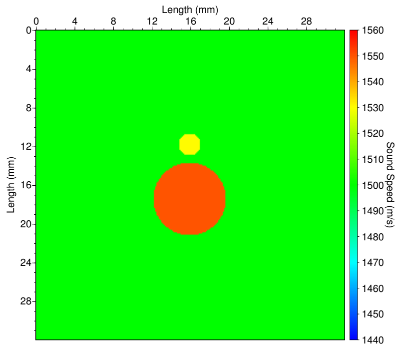

(a) Numerical phantom

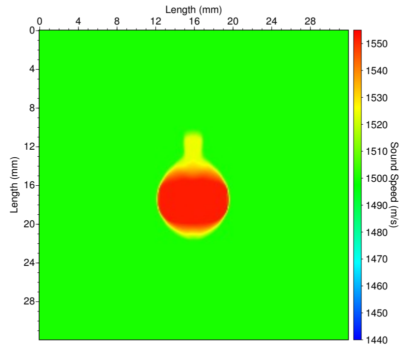

(b) Transmission USWT

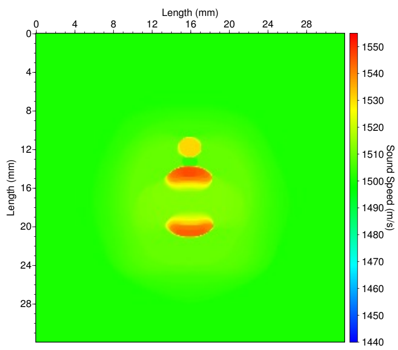

(c) Reflection USWT

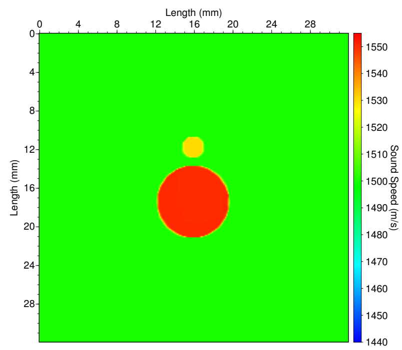

(d) Transmission-reflection USWT

Figure 3: Ultrasound waveform tomography using both ultrasound transmission and reflection data significantly improves tomographic reconstruction compared to those using either transmission or reflection data alone.[45] Numerical synthetic-aperture ultrasound data are generated for two parallel ultrasound transducer arrays on the top and bottom sides of the numerical phantom in (a).

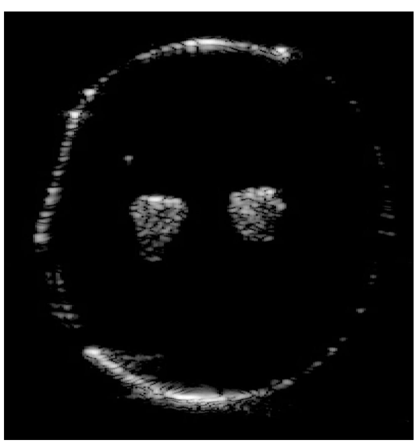

(a) Beamforming using synthetic-aperture ultrasound reflection data

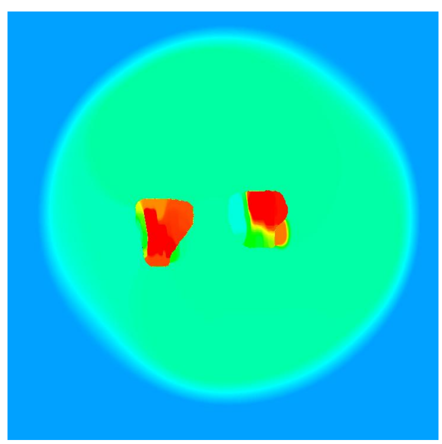

(b) Transmission-reflection ultrasound waveform tomography

Figure 4: Comparison of a beamforming image of a phantom containing two pieces of chicken breast with an ultrasound waveform tomographic reconstruction result of the same phantom. The chicken breast phantom data are acquired using our synthetic-aperture ultrasound tomography system with two parallel transducer arrays (Fig. 1). (From Lin and Huang (2016)[62])

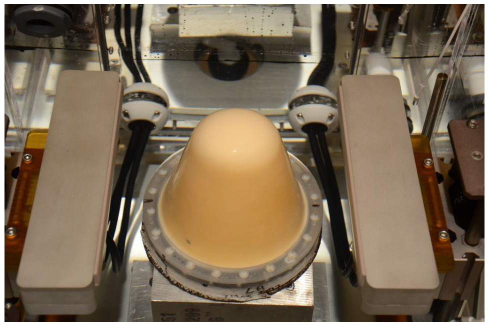

(a) Tissue-mimicking breast phantom

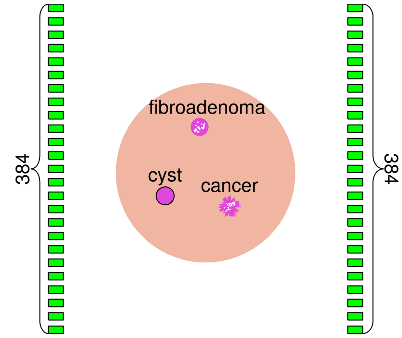

(b) Illustration of one slice of the tissue-mimicking breast phantom in (a)

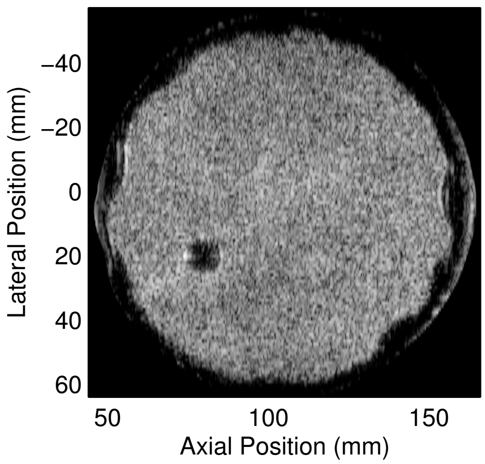

(c) Beamforming using synthetic-aperture ultrasound reflection data

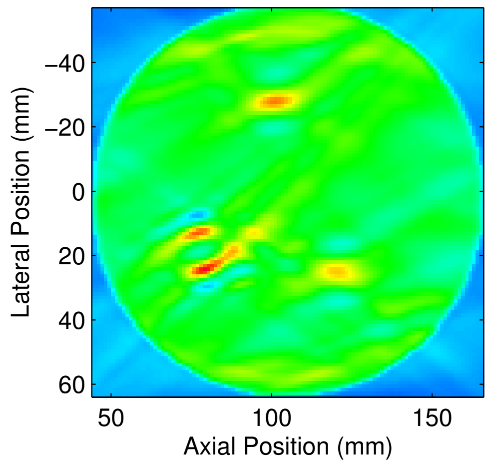

(d) Attenuation tomography using synthetic-aperture ultrasound transmission data

Figure 5: (a) A tissue-mimicking breast phantom manufactured by the University of Wisconsin. (b) Schematic illustration of one slice of the tissue-mimicking breast phantom in (a) scanned using our ultrasound tomography prototype in Fig. 1. (c) Ultrasound beamforming image of a slice of the tissue-mimicking breast phantom in (a) obtained using synthetic-aperture ultrasound reflection data. (d) Ultrasound attenuation tomography result of the same slice of the tissue-mimicking breast phantom obtained using ultrasound transmission data. (From Chen, Shin, and Huang (2016)[57])

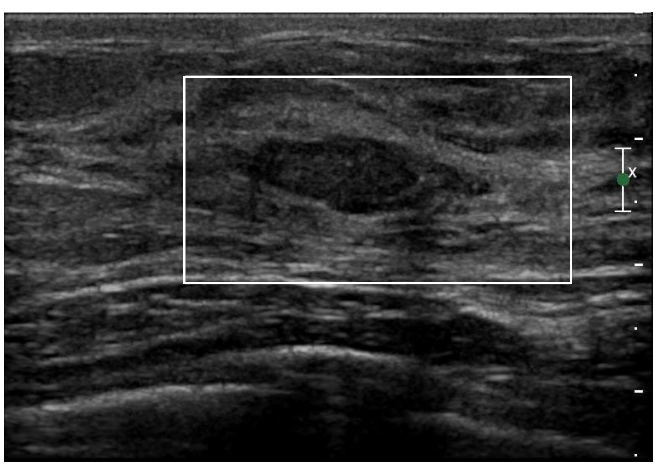

Figure 6: A breast lesion is shown on a clinical ultrasound image of a patient's left breast.

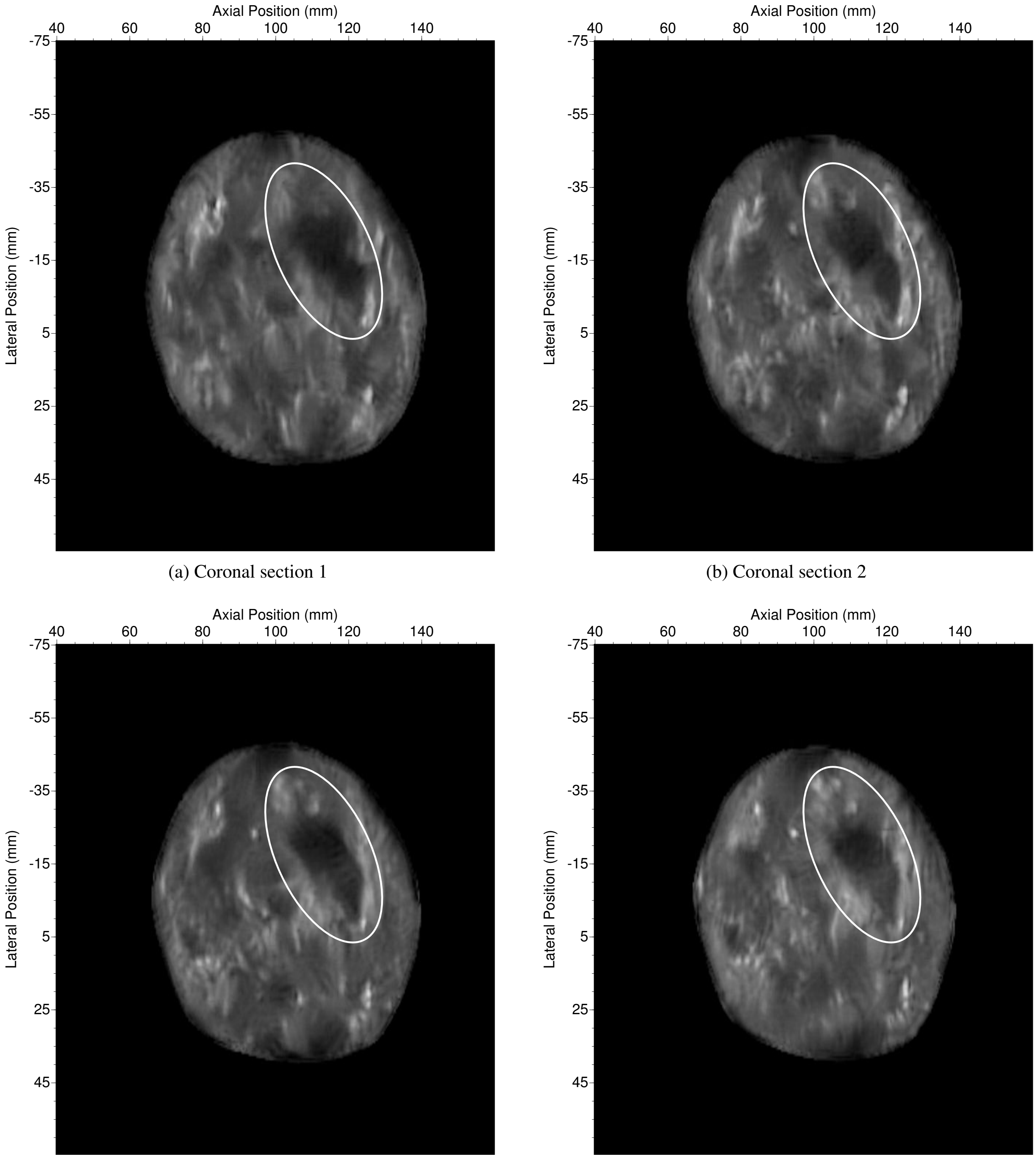

(a) Coronal section 1

(b) Coronal section 2

(c) Coronal section 3

(d) Coronal section 4

Figure 7: Four adjacent coronal sections of ultrasound beamforming images obtained using synthetic-aperture ultrasound data for the patient with a breast lesion as shown in Fig. 6. The breast lesion within the ellipse region in each panel can be clearly identified.

Figure 8: A breast lesion is shown within the circle region on a mammogram of a patient's right breast.

4. ULTRASOUND TRANSMISSION ATTENUATION TOMOGRAPHY

Chen, Shin, and Huang (2016)[57] recently developed an ultrasound attenuation tomography method using ultrasound energy-scaled amplitude decays of ultrasound transmission signals. Our breast phantom imaging and tomography results in Fig. 5 show that our ultrasound attenuation tomography with ultrasound transmission data complements the beamforming image, and is able to detect some breast lesions (low-speed fibroadenoma and low-speed cancer in this case) that are not clearly identified in the beamforming image.

5. *IN VIVO* PATIENT IMAGING

Our clinical collaborator (Radiologist) of the Department of Radiology at the University of New Mexico (UNM) recruited and scanned patients using our synthetic-aperture breast ultrasound tomography prototype under a clinical research protocol approved by the University of New Mexico Institutional Review Board (IRB). Our clinical collaborator recruited patients from the population of patients who undergo work up mammography. These patients may have symptoms or had an abnormal screening mammogram. A total of 29 patients were scanned, and only a few of them had breast lesions.

Patient A was recruited because her left breast had a breast lesion shown on her targeted ultrasound image within a boxed region in Fig. 6. The UNM study personnel scanned Patient A using our breast ultrasound tomography prototype and acquired synthetic-aperture ultrasound transmission and reflection data.

We use the acquired synthetic-aperture ultrasound data to obtain ultrasound beamforming images, and show four adjacent coronal sections of the beamforming images in Fig. 7. In each panel of Fig. 7, the coordinate value zero along the azimuthal/lateral axis is the center position of the two parallel ultrasound transducer arrays, and the both end elements of the two transducer arrays on the head side are at the position of approximately -105 mm. The breast lesion can be clearly identified in the ellipse region in each coronal section in Fig. 7.

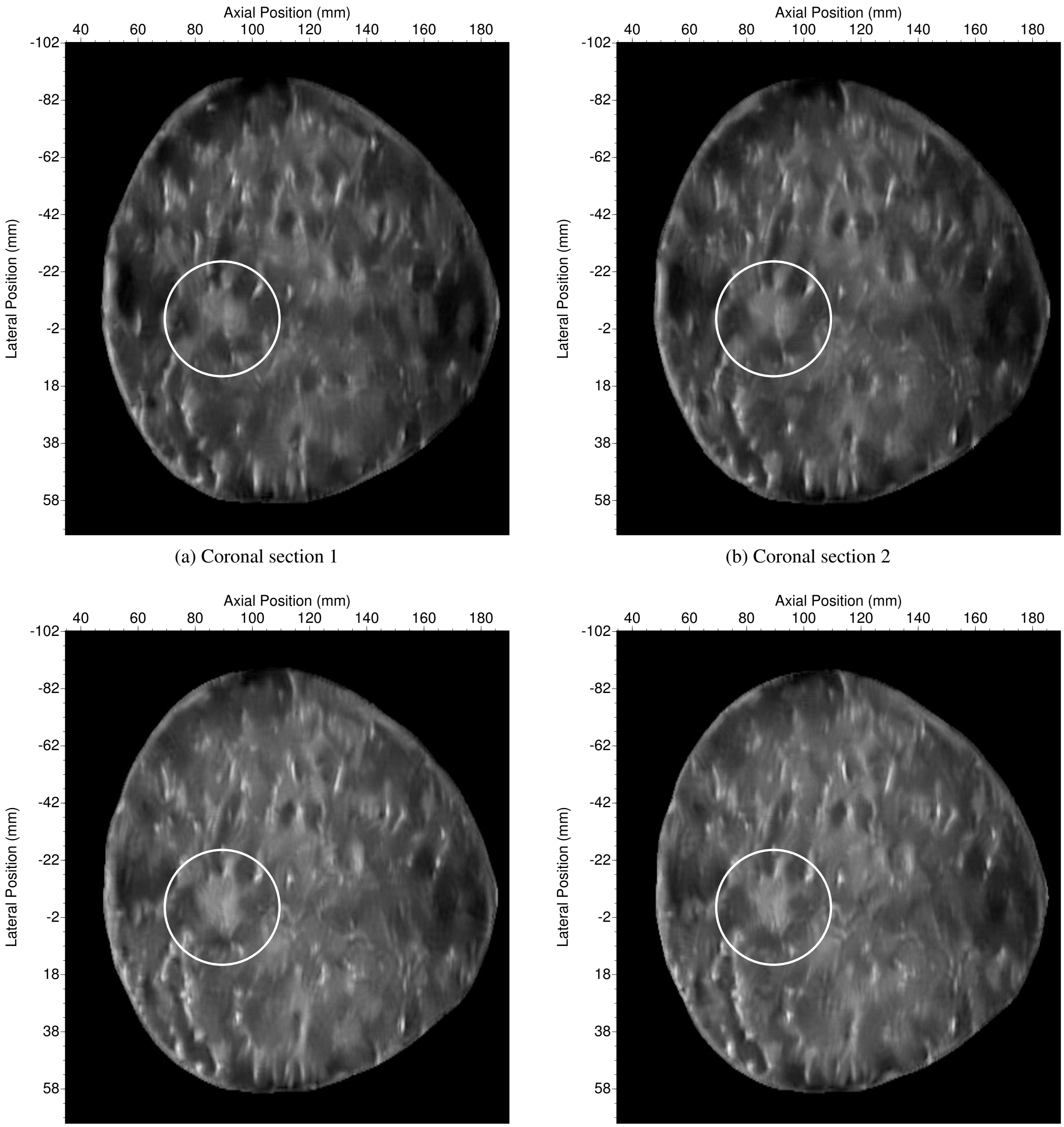

(a) Coronal section 1

(b) Coronal section 2

(c) Coronal section 3

(d) Coronal section 4

Figure 9: Four adjacent coronal sections of ultrasound beamforming images obtained using synthetic-aperture ultrasound data for the patient with a breast lesion as shown in Fig. 8. The breast lesion within the circle region in each panel can be clearly identified.

Patient B was recruited for this study because her right breast had a breast lesion as shown on her mammogram in Fig. 8. Figure 9 displays four adjacent coronal sections of ultrasound beamforming images obtained using synthetic-aperture ultrasound data acquired with our breast ultrasound tomography prototype. The breast lesion is well imaged in each panel of Fig. 9.

6. CONCLUSIONS

We have studied the clinical feasibility of our newly designed and manufactured synthetic-aperture ultrasound tomography prototype with two parallel ultrasound transducer arrays for breast imaging. The prototype consists of two parallel transducer arrays with a total of 768 transducer elements and 384 parallel receive channels. The center frequency of the ultrasound transducer arrays is 1.875 MHz. The distance between the two transducer arrays is adjustable for scanning different sizes of breasts. It takes approximately 2.5 seconds to scan each slice, including times to move the ultrasound transducer arrays, fire all 768 elements sequentially and record all ultrasound reflection and transmission data, and store ultrasound data to solid state hard drives. A total of 40 – 70 slices are normally acquired for each breast, depending on the breast size. We have used the prototype to acquire patient data in a clinical exam room in the building of the University of New Mexico Outpatient Surgery-Imaging Services. Our *in vivo* patient imaging results demonstrate that using our breast ultrasound tomography prototype with two parallel transducer arrays can detect breast lesions shown on clinical patient images obtained with other imaging modalities. Breast ultrasound tomography could become a non-invasive, safe (non-ionizing radiation), comfortable (no compression), and cost-effective modality for breast cancer imaging.

7. ACKNOWLEDGMENTS

This work was supported by the Breast Cancer Research Program of U.S. DOD Congressionally Directed Medical Research Programs. The computation was performed using super-computers of the Institutional Computing Program of Los Alamos National Laboratory. We thank our clinical collaborator Dr. Michael Williamson (M.D., Radiologist) of the Department of Radiology at the University of New Mexico School of Medicine for recruiting patients, acquiring patient ultrasound data and providing clinical patient images. We thank Consumer Advocates Dr. Erin Bouquin (M.D.), Peggy Devine, Elizabeth Harris, and Nancy Hawkins for their support, help, and encouragement during the course of this project.

REFERENCES

[1] Kolb, T. M., Lichy, J., and Newhouse, J. H., "Comparison of the performance of screening mammography, physical examination, and breast us and evaluation of factors that influence them: An analysis of 27,825 patient evaluation," *Radiology* **225**, 165–175 (2002).

[2] Stomper, P. C., D'Souza, D. J., DiNitto, P. A., and Arredondo, M. A., "Analysis of parenchymal density on mammograms in 1353 women 25-79 years old.," *American Journal of Roentgenology* **167**, 1261–1265 (1996).

[3] Kornguth, P. J., Keefe, F. J., and Conaway, M. R., "Pain during mammography: characteristics and relationship to demographic and medical variables," *Pain* **66**(2), 187–194 (1996).

[4] Greenleaf, J., Johnson, S., Lee, S., Hermant, G., and Woo, E., "Algebraic reconstruction of spatial distributions of acoustic absorption within tissue from their two-dimensional acoustic projections," in [*Acoustical Holography*], Green, P., ed., 591–603, Springer US (1974).

[5] Greenleaf, J., Johnson, S., Samayoa, W., and Duck, F., "Algebraic reconstruction of spatial distributions of acoustic velocities in tissue from their time-of-flight profiles," in [*Acoustical Holography*], Booth, N., ed., 71–90, Springer US (1975).

[6] Carson, P. L., Meyer, C. R., Scherzinger, A. L., and Oughton, T. V., "Breast imaging in coronal planes with simultaneous pulse echo and transmission ultrasound," *Science* **214**, 1141–1143 (1981).

[7] Waag, R. C., Liu, D.-L., Mast, T. D., Nachman, A. I., Jaeger, P., and Kojima, T., "An ultrasonic ring transducer system for studies of scattering and imaging," *J. Acoust. Soc. Am.* **100**, 2795 (1996).

[8] Andre, M. P., Janee, H. S., Martin, P. J., Otto, G. P., Spivey, B. A., and Palmer, D. A., "High-speed data acquisition in a diffraction tomography system employing large-scale toroidal arrays," *International Journal of Imaging Systems and Technology* **8**, 137–147 (1997).

[9] Wiskin, J. W., Borup, D. T., and Johnson, S. A., "Inverse scattering from arbitrary two-dimensional objects in stratified environments via a green's operator," *Journal of the Acoustical Society of America* **102**, 853–864 (1997).

[10] Marmarelis, V. Z., Kim, T. S., and Shehada, R. E. N., "High resolution ultrasonic transmission tomography," in [*Ultrasonic Imaging and Signal Processing*], Walker, W. F. and Insana, M. F., eds., *Proc. SPIE* **5035**, 33–40, SPIE, Bellingham, Washington (2002).

[11] Duric, N., Littrup, P., Poulo, L., Babkin, A., Pevzner, R., Holsapple, E., and Rama, O., "Detection of breast cancer with ultrasound tomography: First results with the computerized ultrasound risk evaluation (cure) prototype," *Med. Phys.* **34**, 773–785 (2007).

[12] Duric, N., Littrup, P., Roy, O., Li, C., Schmidt, S., Cheng, X., and Janer, R., "Clinical breast imaging with ultrasound tomography: A description of the softvue system," *The Journal of the Acoustical Society of America* **135**(4), 2155–2155 (2014).

[13] Ruiter, N. V., Zapf, M., Hopp, T., Dapp, R., Kretzek, E., Birk, M., Kohout, B., and Gemmeke, H., "3d ultrasound computer tomography of the breast: A new era?," *European Journal of Radiology* **81**, S133–134 (2012).

[14] Huang, L., Shin, J., Chen, T., Lin, Y., Intrator, M., Hanson, K., Epstein, K., Sandoval, D., , and Williamson, M., "Breast ultrasound tomography with two parallel transducer arrays: Preliminary clinical results," in [*Ultrasonic Imaging and Tomography*], Bosch, J. G. and Duric, N., eds., *Proc. SPIE* **9419**, 941916–1–10, SPIE, Bellingham, Washington (2015).

[15] O'Donnell, M. and Thomas, L. J., "Efficient synthetic aperture imaging from a circular aperture with possible application to catheter-based imaging," *IEEE Transactions on Ultrasonics, Ferroelectrics, and Frequency Control* **39**, 366–380 (1992).

[16] Lockwood, G., Talman, J., and Brunke, S., "Real-time 3-d ultrasound imaging using sparse synthetic aperture beamforming," *IEEE Trans. Ultrason. Ferroelectr. Freq. Control* **45**, 980–988 (1998).

[17] Nikolov, S., Gammelmark, K., and Jensen, J., "Recursive ultrasound imaging," *Proceedings of the IEEE Ultrasonic Symposium* **2**, 1621–1625 (1999).

[18] Nikolov, S. I., *Synthetic aperture tissue and flow ultrasound imaging*, PhD thesis, Technical University of Denmark (2001).

[19] Jensen, J., Holm, O., Jensen, L., Bendsen, H., Nikolov, S., Tomov, B., Munk, P., Hansen, M., Salomonsen, K., Hansen, J., Gormsen, K., Pedersen, H., and Gammelmark, K., "Ultrasound research scanner for real-time synthetic aperture data acquisition," *IEEE Trans. Ultrason. Ferroelectr. Freq. Control* **52**, 881–891 (2005).

[20] Huang, L., Duric, N., and Littrup, P., "Breast imaging with time-reversed ultrasound," *Proc. SPIE* **6147**, 156–167 (2006).

[21] Jensen, J., Nikolov, S., Gammelmark, K., and Pedersen, M., "Synthetic aperture ultrasound imaging," *Ultrasonics* **44**, e5–e15 (2006).

[22] Daher, N. and Yen, J., "2-d array for 3-d ultrasound imaging using synthetic aperture techniques," *IEEE Trans. Ultrason. Ferroelectr. Freq. Control* **53**, 912–924 (2006).

[23] Huang, L., Duric, N., and Littrup, P., "Ultrasonic breast imaging using a wave-equation migration method," *Proc. SPIE* **5035**, 432–439 (2003).

[24] Simonetti, F., "Multiple scattering: The key to unravel the subwavelength world from the far-field pattern of a scattered wave," *Physical Review E* **73**, 036619–1–13 (2006).

[25] Huang, L. and Quan, Y., "Ultrasound pulse-echo imaging using the split-step Fourier propagator," *Proc. SPIE* **6513**, 651305–1–12 (2007).

[26] Pratt, R. G., Huang, L., Duric, N., and Littrup, P., "Sound-speed and attenuation of the breast tissue using waveform tomography of transmission ultrasound data," in [*Physics of Medical Imaging*], Hsieh, J. and Flynn, M. J., eds., *Proc. SPIE* **6510**, 65104S–1–12, SPIE, Bellingham, Washington (2007).

[27] Simonetti, F., Huang, L., Duric, N., and Rama, O., "Imaging beyond the born approximation: An experimental investigation with an ultrasonic ring array," *Physical Review E* **76**, 036601–1–10 (2007).

[28] Simonetti, F. and Huang, L., "From beamforming to diffraction tomography," *Journal of Applied Physics* **103**, 103110–1–7 (2008).

[29] Huang, L., Hanson, K. M., Quan, Y., Li, C., and Duric, N., "Globally optimized Fourier finite-difference method for ultrasound breast imaging," *Proc. SPIE* **6920**, 692007–1–11 (2008).

[30] Andresen, H., Nikolov, S., Pedersen, M., Buckton, D., and Jensen, J., "Three-dimensional synthetic aperture focusing using a rocking convex array transducer," *IEEE Trans. Ultrason. Ferroelectr. Freq. Control* **57**, 1051–1063 (2010).

[31] Huang, L., Simonetti, F., Huthwaite, P., Rosenberg, R., and Williamson, M., "Detecting breast microcalcifications using super-resolution and wave-equation ultrasound imaging: A numerical phantom study," in [*Ultrasonic Imaging, Tomography, and Therapy*], D'hooge, J. and McAleavey, S. A., eds., *Proc. SPIE* **7629**, 762919–1–10, SPIE (2010).

[32] Nikolov, S. I., Kortbek, J., and Jensen, J. A., "Practical applications of synthetic aperture imaging," in [*Proceedings – IEEE Ultrasonics Symposium*], 350–358 (2010).

[33] Huang, L., Labyed, Y., Simonetti, F., Williamson, M., Rosenberg, R., Heintz, P., and Sandoval, D., "High-resolution imaging with a real-time synthetic aperture ultrasound system: A phantom study," in [*Ultrasonic Imaging, Tomography, and Therapy*], D'hooge, J. and Doyley, M. M., eds., *Proc. SPIE* **7968**, 79681I–1–10, SPIE (2011).

[34] Labyed, Y. and Huang, L., "Detecting small targets using windowed time-reversal MUSIC imaging: A phantom study," *International Ultrasonics Symposium Proceedings* **10.1109/ULTSYM.2011.0392**, 1579–1582 (2011).

[35] Huang, L., Labyed, Y., Lin, Y., Zhang, Z., Pohl, J., Sandoval, D., and Williamson, M., "Detection of breast microcalcifications using synthetic-aperture ultrasound," in [*Ultrasonic Imaging, Tomography, and Therapy*], D'hooge, J. and Doyley, M. M., eds., *Proc. SPIE* **8320**, 83200H–1–8, SPIE (2012).

[36] Labyed, Y. and Huang, L., "Ultrasound imaging of extended targets using a windowed time-reversal MUSIC method," in [*Ultrasonic Imaging, Tomography, and Therapy*], D'hooge, J. and Doyley, M. M., eds., *Proc. SPIE* **8320**, 832019–1–10, SPIE (2012).

[37] Labyed, Y. and Huang, L., "Ultrasound time-reversal MUSIC imaging with diffraction and attenuation compensation," *IEEE Trans. Ultrason. Ferroelectr. Freq. Control* **59**, 2186–2200 (2012).

[38] Labyed, Y. and Huang, L., "Ultrasound time-reversal MUSIC imaging of extended targets," *Ultrasound in Med. & Biol.* **38**, 2018–2030 (2012).

[39] Huang, L., Labyed, Y., Hanson, K., Sandoval, D., Pohl, J., and Williamsonb, M., "Detecting breast microcalcifications using super-resolution ultrasound imaging: A clinical study," in [*Ultrasonic Imaging, Tomography, and Therapy*], Bosch, J. G. and Doyley, M. M., eds., *Proc. SPIE* **8675**, doi: 10.1117/12.2007653, 86751O–1–10, SPIE, Bellingham, Washington (2013).

[40] Labyed, Y. and Huang, L., "Super-resolution ultrasound phase-coherent MUSIC imaging with compensation for the phase response of transducer elements," *IEEE Trans. Ultrason. Ferroelectr. Freq. Control* **60**, 1048–1060 (2013).

[41] Labyed, Y. and Huang, L., "TR-MUSIC inversion of the density and compressibility contrasts of point scatterers," *IEEE Transactions on Ultrasonics, Ferroelectrics, and Frequency Control* **61**, 16–24 (2014).

[42] Lin, Y. and Huang, L., "Ultrasound waveform tomography with a spatially-variant regularization scheme," in [*Ultrasonic Imaging and Tomography*], Bosch, J. G. and Doyley, M. M., eds., *Proc. SPIE* **9040**, 90401M–1–7, SPIE, Bellingham, Washington (2014).

[43] Nguyen, N. Q. and Huang, L., "Ultrasound bent-ray tomography using both transmission and reflection data," in [*Ultrasonic Imaging and Tomography*], Bosch, J. G. and Doyley, M. M., eds., *Proc. SPIE* **9040**, 90400R–1–8, SPIE, Bellingham, Washington (2014).

[44] Labyed, Y. and Huang, L., "Toward real-time bent-ray breast ultrasound tomography using gpus," in [*Ultrasonic Imaging and Tomography*], Bosch, J. G. and Doyley, M. M., eds., *Proc. SPIE* **9040**, 90401N–1–8, SPIE, Bellingham, Washington (2014).

[45] Huang, L., Lin, Y., Zhang, Z., Labyed, Y., Tan, S., Nguyen, N., Hansona, K., Sandoval, D., and Williamson, M., "Breast ultrasound waveform tomography: Using both transmission and reflection data, and numerical virtual point sources," in [*Ultrasonic Imaging and Tomography*], Bosch, J. G. and Doyley, M. M., eds., *Proc. SPIE* **9040**, 90400T–1–12, SPIE, Bellingham, Washington (2014).

[46] Zhang, Z. and Huang, L., "Efficient implementation of ultrasound waveform tomography using data blending," in [*Ultrasonic Imaging and Tomography*], Bosch, J. G. and Doyley, M. M., eds., *Proc. SPIE* **9040**, 90401O–1–9, SPIE, Bellingham, Washington (2014).

[47] Littrup, P. J., Duric, N., Azevedo, S., Chambers, D. H., Candy, J. V., Johnson, S., Auner, G., Rather, J., and Holsapple, E. T., "Computerized Ultradound Risk Evaluation (CURE) system: Development of combined transmission and reflection ultrasound with new reconstruction algorithms for breast imaging," *Acoustical Imaging* **26**, 175–182 (2002).

[48] Littrup, P., Duric, N., Leach Jr., R. R., Azevedo, S. G., Candy, J. V., Moore, T., Chambers, D. H., Mast, J. E., and Holsapple, E. T., "Characterizing tissue with acoustic parameters derived from ultrasound data," in [*Ultrasonic Imaging and Signal Proceesing*], Insana, M. and Walker, W. F., eds., *Proc. SPIE* **4687**, 354–361, SPIE, Bellingham, Washington (2002).

[49] Duric, N., Littrup, P., Holsapple, E. T., Babkin, A., Duncan, R., Kalinin, A., Pevzner, R., and Tokarev, M., "Ultrasound tomography of breast tissue," in [*Ultrasonic Imaging and Signal Processing*], Walker, W. F. and Insana, M., eds., *Proc. SPIE* **5035**, SPIE, Bellingham, Washington (2003).

[50] Duric, N., Littrup, P. J., Rama, O., and Holsapple, E. T., "Computerized ultrasound risk evaluation (CURE): First clinical results," *Acoustical Imaging* **28** (2005).

[51] Quan, Y. and Huang, L., "Sound-speed tomography using first-arrival transmission ultrasound for a ring array," in [*Ultrasonic Imaging and Signal Processing*], Emelianov, S. Y. and McAleavey, S. A., eds., *Proc. SPIE* **6513**, doi: 10.1117/12.709647, 651306–1–9, SPIE, Bellingham, Washington (2007).

[52] Li, C., Duric, N., and Huang, L., "Clinical breast imaging using sound-speed reconstructions of ultrasound tomography data," in [*Ultrasonic Imaging and Signal Processing*], McAleavey, S. A. and D'hooge, J., eds., *Proc. SPIE* **6920**, 692009–1–9, SPIE (2008).

[53] Li, C., Duric, N., and Huang, L., "Comparison of ultrasound attenuation tomography methods for breast imaging," in [*Ultrasonic Imaging and Signal Processing*], McAleavey, S. A. and D'hooge, J., eds., *Proc. SPIE* **6920**, 692015–1–9, SPIE (2008).

[54] Li, C., Duric, N., Littrup, P., and Huang, L., "In vivo breast sound-speed imaging with ultrasound tomography," *Untrasound in Med. & Biol.* **35**, 1615–1628 (2009).

[55] Li, C., Huang, L., Duric, N., Zhang, H., and Rowe, C., "An improved automatic time-of-flight picker for medical ultrasound tomography," *Ultrasonics* **49**, 61–72 (2009).

[56] Intrator, M., Lin, Y., Chen, T., Shin, J., and Huang, L., "Ultrasound bent-ray tomography with a modified total-variation regularization scheme," in [*Ultrasonic Imaging and Tomography*], Bosch, J. G. and Duric, N., eds., *Proc. SPIE* **9419**, 941917–1–10, SPIE, Bellingham, Washington (2015).

[57] Chen, T., Shin, J., and Huang, L., "Ultrasound transmission attenuation tomography using energy-scaled amplitude ratios," in [*Ultrasonic Imaging and Tomography*], *Proc. SPIE* **9790**, SPIE, Bellingham, Washington (2016).

[58] Lin, Y., Huang, L., and Zhang, Z., "Ultrasound waveform tomography with the total-variation regularization for detection of small breast tumors," in [*Ultrasonic Imaging, Tomography, and Therapy*], Bosch, J. G. and Doyley, M. M., eds., *Proc. SPIE* **8320**, doi: 10.1117/12.910765, 832002–1–9, SPIE, Bellingham, Washington (2012).

[59] Zhang, Z., Huang, L., and Lin, Y., "Efficient implementation of ultrasound waveform tomography using source encoding," in [*Ultrasonic Imaging, Tomography, and Therapy*], Bosch, J. G. and Doyley, M. M., eds., *Proc. SPIE* **8320**, doi: 10.1117/12.910969, 832003–1–10, SPIE, Bellingham, Washington (2012).

[60] Lin, Y. and Huang, L., "Ultrasound waveform tomography with a modified total-variation regularization scheme," in [*Ultrasonic Imaging, Tomography, and Therapy*], Bosch, J. G. and Doyley, M. M., eds., *Proc. SPIE* **8675**, doi: 10.1117/12.2007650, 86751F–1–9, SPIE, Bellingham, Washington (2013).

[61] Zhang, Z. and Huang, L., "Ultrasound waveform tomography using wave-energy-based preconditioning," in [*Ultrasonic Imaging, Tomography, and Therapy*], Bosch, J. G. and Doyley, M. M., eds., *Proc. SPIE* **8675**, doi: 10.1117/12.2007659, 86751G–1–10, SPIE, Bellingham, Washington (2013).

[62] Lin, Y. and Huang, L., "Ultrasound waveform tomography with the second-order total-generalized-variation regularization," in [*Physics of Medical Imaging*], *Proc. SPIE* **9783**, SPIE, Bellingham, Washington (2016).